Electronic supplementary information for:

Reaching the 5% theoretical limit of fluorescent OLEDs with push-pull benzophospholes

Nicolas Ledos,[a] Denis Tondelier,[b] Bernard Geffroy,[c] Denis Jacquemin,*[d,e] Pierre-Antoine Bouit*[a] and Muriel Hissler*[a]

[a] Univ Rennes, CNRS, ISCR - UMR 6226, F-35000 Rennes, pierre-antoine.bouit@univ-rennes.fr, muriel.hissler@univ-rennes.fr

[b] LPICM, CNRS, Ecole Polytechnique, Institut Polytechnique de Paris, route de Saclay, 91128 Palaiseau, France

[c] Université Paris-Saclay, CEA, CNRS, NIMBE, LICSEN, 91191, Gif-sur-Yvette, France

[d] Nantes Université, CNRS, CEISAM UMR 6230, F-44300, Nantes, France, denis.jacquemin@univ-nantes.fr

[e] Institut Universitaire de France, F-75005 Paris, France.

Table of Content

Experimental Part.

All experiments were performed under an atmosphere of dry argon using standard Schlenk techniques. Commercially available reagents were used as received without further purification. Solvents were freshly purified using MBRAUN SPS-800 drying columns. Separations were performed by gravity column chromatography on silica gel (ACROS Organic Silica gel, for column chromatography, 0.035-0.070mm, 60Å)

^{1}H, ^{13}C, and ^{31}P NMR spectra were recorded on Bruker AV 300 and AV III 400 MHz NMR spectrometers equipped with BBO or BBFO probeheads.

Assignment of proton and carbon atoms is based on COSY, edited-HSQC and HMBC experiments. ^{1}H and ^{13}C NMR chemical shifts were reported in parts per million (ppm) using residual solvent signal as reference. In the NMR description, Cq corresponds to quaternary carbon. High-resolution mass spectra were obtained on a Varian MAT 311 or ZabSpec TOF Micromass instrument at CRMPO (Scanmat, UMS 2001). UV-Visible spectra were recorded at room temperature on a Specord 205 UV/Vis/NIR spectrophotometer. The UV-Vis emission and excitation spectra measurements were recorded on a FL 920 Edimburgh Instrument equipped with a Hamamatsu R5509-73 photomultiplier for the NIR domain (300-1700 nm) and corrected for the response of the photomultiplier. Quantum yields were calculated relative to fluorescein (NaOH, 0.1 M), ϕref= 0.79. The absolute quantum yields were measured with a C9920-03 Hamamatsu. Life-times measurements were conducted with 375 nm diode laser excitation (EPL-series) plugged to a TCSPC pulsed source interface using an Edinburgh FS920 Steady State Fluorimeter combined with a FL920 Fluorescence Lifetime Spectrometer. The electrochemical studies were carried out under argon using an Eco Chemie Autolab PGSTAT 30 potentiostat for cyclic voltammetry with the three-electrode configuration: the working electrode was a platinum disk, the reference electrode was a saturated calomel electrode and the counter-electrode a platinum wire. All potentials were internally referenced to the ferrocene/ ferrocenium couple. For the measurements, concentrations of 10^{-3} M of the electroactive species were used in freshly distilled and degassed dichloromethane and 0.2 M tetrabutylammonium hexafluorophosphate. Thermogravimetric Analysis and Differential Scanning Calorimetry were performed by using a Mettler-Toledo TGA-DSC-1 apparatus under dry nitrogen flow at a heating rate of 10 °C/min. Ethyl phenylphosphinate was synthesized following a reported procedure.[1]

Synthesis of 4,4'-(ethyne-1,2-diyl)bis(N,N-diphenylaniline): (1,2-Bis(4-bromophenyl)ethyne (500 mg, 1.48 mmol), diphenylamine (550 mg, 3.25 mmol), *t*BuOK(1 g, 8.9mmol), acetic acid palladium (II) (32 mg, 0.14 mmol) and Tri-*tert*-butylphosphonium tetrafluoroborate (125 mg, 0.42 mmol) were added into a Schlenk and three Argon-vacuum cycles were performed. Then the Schlenk was filled up with 40 mL of degassed toluene. Subsequently, the mixture was heated to 120°C overnight, and then cooled to rt. After removing the solvent in vacuum, the mixture was partitioned between DCM and water. The combined organic layers were washed with brine, dried over Mg_2SO_4 and purified by column chromatography on silica gel (eluent: DCM/Pentane = 30/70), affording a yellow solid in 83% yield (625 mg). ^{1}H NMR (400 MHz, $CDCl_3$) δ 7.39 – 7.32 (m, 4H), 7.31 – 7.22 (m, 8H), 7.15 – 7.08 (m, 8H), 7.05 (t, J = 7.3 Hz, 4H), 7.00 (d, J = 8.7 Hz, 4H). NMR data fit with previously reported procedure.[2]

Synthesis of 4,4'-(ethyne-1,2-diyl)bis(N,N-bis(4-methoxyphenyl)aniline): (1,2-Bis(4-bromophenyl)ethyne (600 mg, 1.79 mmol), bis(4-methoxyphenyl)amine (900 mg, 3.93 mmol), *t*BuOK(1.2 g, 10.7 mmol), acetic acid palladium (II) (40 mg, 0.18 mmol) and Tri-*tert*-butylphosphonium tetrafluoroborate (150 mg, 0.5 mmol) were added into a Schlenk and three Argon-vacuum cycles were performed. Then the Schlenk was filled up with 40 mL of degassed toluene. Subsequently, the mixture was heated to 120°C overnight, and then cooled to rt. After removing the solvent in vacuum, the mixture was partitioned between DCM and water. The combined organic layers were washed with brine, dried over Mg_2SO_4 and purified by column chromatography on silica gel (eluent: DCM/Pentane = 1/1), affording a yellow solid in 94% yield (1.06 g). ^{1}H NMR (400 MHz, CD_2Cl_2) δ 7.25 (d, J = 8.8 Hz, 4H), 7.11 – 7.02 (m, 8H), 6.89 – 6.82 (m, 8H), 6.80 (d, J = 8.8 Hz, 4H), 3.78 (s, 12H). NMR data fit with previously reported procedure.[3]

Synthesis of 1,2-bis(4-(10H-phenoxazin-10-yl)phenyl)ethyne: (1,2-Bis(4-bromophenyl)ethyne (450 mg, 1.34 mmol), 10H-phenoxazine (540mg, 2.96 mmol), *t*BuOK(0.9 g, 8mmol), acetic acid palladium (II) (30 mg, 0.13 mmol) and Tri-*tert*-butylphosphonium tetrafluoroborate (113 mg, 0.39 mmol) were added into a Schlenk and three Argon-vacuum cycles were performed. Then the Schlenk was filled up with 30 mL of degassed toluene. Subsequently, the mixture was heated to 120°C overnight, and then cooled to rt. After removing the solvent in vacuum, the mixture was partitioned between DCM and water. The combined organic layers were washed with brine, dried over Mg_2SO_4 and purified by column chromatography on silica gel (eluent: DCM/Pentane = 1/2), affording a yellow solid in 73% yield (500 mg).
^{1}H NMR (400 MHz, $CDCl_3$) δ 7.78 (d, *J* = 8.4 Hz, 4H), 7.37 (d, *J* = 8.4 Hz, 4H), 6.75 – 6.55 (m, 12H), 5.97 (d, *J* = 7.8 Hz, 4H). NMR data fit with previously reported procedure.[4]

General Procedure for Benzophospholes synthesis: A mixture of the corresponding alkyne (1eq), ethyl phenylphosphinate (2eq), and Ag_2O (2eq,) in DMF was stirred at 120°C under Ar overnight. After cooling to rt, the mixture was diluted with ethyl acetate (30 mL) and the insoluble solids were removed on a Celite plug. The filtrate was transferred in a round bottom flask and 2mL of hydrogen peroxide were added and the solution was stirred for 30 minutes. The solution was washed with water and brine and dried over anhydrous Mg_2SO_4. After filtration, the solvent was evaporated under reduced pressure, and the residue was purified by column chromatography on silica gel by using DCM/ethyl acetate (95/5 v/v) as eluent to afford the product.

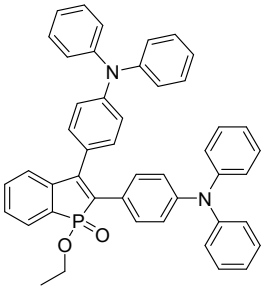

2a was synthesized according to general procedure starting from 500 mg of 4,4'-(ethyne-1,2-diyl)bis(N,N-diphenylaniline). 1 was obtained as a yellow solid (m = 266 mg Yield = 40%)

^{1}H NMR (300 MHz, CD_2Cl_2) δ 7.69 (dd, *J* = 10.3, 7.0 Hz, 1H), 7.53 – 7.45 (m, 1H), 7.43 – 7.36 (m, 1H), 7.33 – 7.22 (m, 10H), 7.23 (dd, *J* = 7.7, 3.5 Hz, 1H), 7.19 – 7.03 (m, 16H), 6.90 (d, *J* = 8.6 Hz, 2H), 4.15 – 3.90 (m, 2H), 1.25 (t, *J* = 7.0 Hz, 3H). ^{13}C NMR (75 MHz, CD_2Cl_2) δ 148.7 (C_q), 148.1 (C_q), 147.9 (C_q), 147.8 (C_q), 147.3 (d, *J(C-P)* = 28 Hz, C_q(β)), 143.0 (d, *J(C-P)* = 34 Hz, C_q(β)), 133.5 (d, *J(C-P)* = 2 Hz, *CH*), 130.5 (s, *CH*), 130.4 (d, *J(C-P)* = 7 Hz, *CH*), 130.0 (s, *CH*), 129.9 (s, *CH*), 129.3 (d, *J(C-P)* = 111 Hz, C_q(α)), 129.2 (d, *J(C-P)* = 11 Hz, *CH*), 128.0 (d, *J(C-P)* = 19 Hz, C_q), 127.9 (d, *J(C-P)* = 9 Hz, *CH*), 127.6 (d, *J(C-P)* = 118 Hz, C_q(α)), 126.6 (d, *J(C-P)* = 10 Hz, C_q), 125.6 (s, *CH*), 125.4 (s, *CH*), 124.3 (s, *CH*), 124.1 (s, *CH*), 124.0 (s, *CH*), 123.4 (s, *CH*), 122.4 (s, *CH*), 62.6 (d, *J(C-P)* = 6 Hz, O*CH*$_2$), 16.8 (d, *J(C-P)* = 6 Hz, *CH*$_3$). ^{31}P NMR (162 MHz, CD_2Cl_2) δ +45.5 (s). HRMS (ESI, CH_2Cl_2): $[M]^+$($C_{46}H_{37}N_2O_2P$), m/z Calcd for: 680.2593, m/z Found: 680.2585. Anal. Calcd for $C_{46}H_{37}N_2O_2P$: C, 81.16; H, 5.48; N, 4.11. Found: C, 79.91; H, 5.44; N, 3.89.

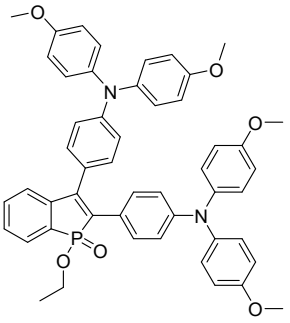

2b was synthesized according to general procedure starting from 500 mg of 4,4'-(ethyne-1,2-diyl)bis(N,N-bis(4-methoxyphenyl)aniline). 2 was obtained as an orange solid (m = 196 mg Yield = 31%)

^{1}H NMR (300 MHz, CD_2Cl_2) δ 7.70 (dd, *J* = 10.3, 7.1 Hz, 1H), 7.55 – 7.45 (m, 1H), 7.44 – 7.35 (m, 1H), 7.33 – 7.20 (m, 3H), 7.18 – 7.06 (m, 10H), 7.00 – 6.84 (m, 10H), 6.77 (d, *J* = 8.7 Hz, 2H), 4.15 – 3.94 (m, 2H), 3.83 (s, 12H), 1.28 (t, *J* = 7.1 Hz, 3H). ^{13}C NMR (101 MHz, CD_2Cl_2) δ 156.4 (C_q), 156.3 (C_q), 149.0 (C_q), 148.4 (C_q), 146.0 (d, *J*(C-P) = 28 Hz, C_q(β)), 142.9 (d, *J(C-P)* = 34 Hz, C_q(β)), 140.3 (C_q), 140.1 (C_q), 132.8 (d, *J(C-P)* = 2 Hz, *CH*), 129.7 (s, *CH*), 129.6 (d, *J(C-P)* = 7 Hz, *CH*), 128.3 (d, *J(C-P)* = 105 Hz, C_q(α)), 128.2 (d, *J(C-P)* = 11 Hz, *CH*), 127.4 (s, *CH*), 127.2 (s, *CH*), 127.1 (s, *CH*), 127.0 (d, *J(C-P)* = 115 Hz, C_q(α)), 125.4 (d, *J(C-P)* = 18 Hz, C_q), 124.0 (d, *J(C-P)* = 10 Hz, C_q), 123.4 (d, *J(C-P)* = 13 Hz, *CH*), 119.3 (s, *CH*), 118.5 (s, *CH*), 114.7 (s, *CH*), 114.6 (s, *CH*), 61.9 (d, *J(C-P)* = 6 Hz, *OCH*$_2$), 55.4 (s, *OCH*$_3$), 16.3 (d, *J(C-P)* = 6 Hz, *CH*$_3$). ^{31}P NMR (162 MHz, CD_2Cl_2) δ +46.0 (s). HRMS (ESI, CH_2Cl_2): $[M]^+$($C_{50}H_{45}N_2O_6P$), m/z Calcd for: 800.3015, m/z Found: 800.3004. Anal. Calcd for $C_{50}H_{45}N_2O_6P$: C, 74.99; H, 5.66; N, 3.50. Found: C, 74.11; H, 5.69; N, 3.20.

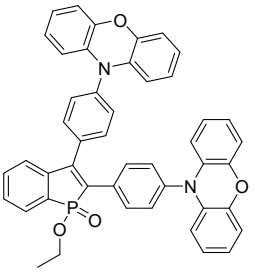

2c was synthesized according to general procedure starting from 500 mg of 1,2-bis(4-(10H-phenoxazin-10-yl)phenyl)ethyne. 3 was obtained as an orange solid (m = 243 mg Yield = 37%).

^{1}H NMR (400 MHz, CD_2Cl_2) δ 7.84 – 7.78 (m, 1H), 7.68 – 7.62 (m, 2H), 7.61 – 7.55 (m, 3H), 7.55 – 7.49 (m, 1H), 7.47 (d, *J* = 8.5 Hz, 2H), 7.27 (d, *J* = 8.4 Hz, 3H), 6.73 – 6.51 (m, 12H), 5.95 (ddd, *J* = 21.3, 7.9, 1.3 Hz, 4H), 4.25 – 4.06 (m, 2H), 1.32 (t, *J* = 7.0 Hz, 3H). 13C NMR (101 MHz, CD_2Cl_2) δ 149.6 (d, *J(C-P)* = 27 Hz, C_q(β)), 144.5 (C_q), 144.4 (C_q), 141.8 (d, *J(C-P)* = 33 Hz, C_q(β)), 140.1 (C_q), 139.3 (C_q), 134.7 (C_q), 134.6 (C_q), 134.5 (d, *J(C-P)* = 18 Hz, C_q), 133.8 (d, *J(C-P)* = 2 Hz, *CH*), 133.5 (d, *J(C-P)* = 9 Hz, C_q), 132.5 (s, *CH*), 132.3 (d, *J(C-P)* = 5 Hz, *CH*), 132.2 (s, *CH*), 131.3 (s, *CH*), 130.9 (d, *J(C-P)* = 125 Hz, C_q(α)), 130.1 (d, *J(C-P)* = 11 Hz, *CH*), 127.9 (d, *J(C-P)* = 133 Hz, C_q(α)), 128.4 (d, *J(C-P)* = 9 Hz, *CH*), 124.6 (d, *J(C-P)* = 13 Hz, *CH*), 124.0 (s, *CH*), 123.9 (s, *CH*), 122.1 (s, *CH*), 122.0 (s, *CH*), 116.0 (s, *CH*), 115.9 (s, *CH*), 113.8 (s, *CH*), 113.7 (s, *CH*), 63.0 (d, *J(C-P)* = 7 Hz, *OCH*$_2$), 16.9 (d, *J(C-P)* = 6 Hz, *CH*$_3$). ^{31}P NMR (162 MHz, CD_2Cl_2) δ +44.0 (s). HRMS (ESI, CH_2Cl_2/CH_3OH;

90/10): $[M+Na]^+$($C_{46}H_{33}N_2O_4PNa$), m/z Calcd for: 731.2070, m/z Found: 731.2071. (MAXI 4G). Anal. Calcd for $C_{46}H_{33}N_2O_4P$: C, 77.95; H, 4.69; N, 3.95. Found: C, 77.75; H, 4.94; N, 3.72.

NMR Spectra

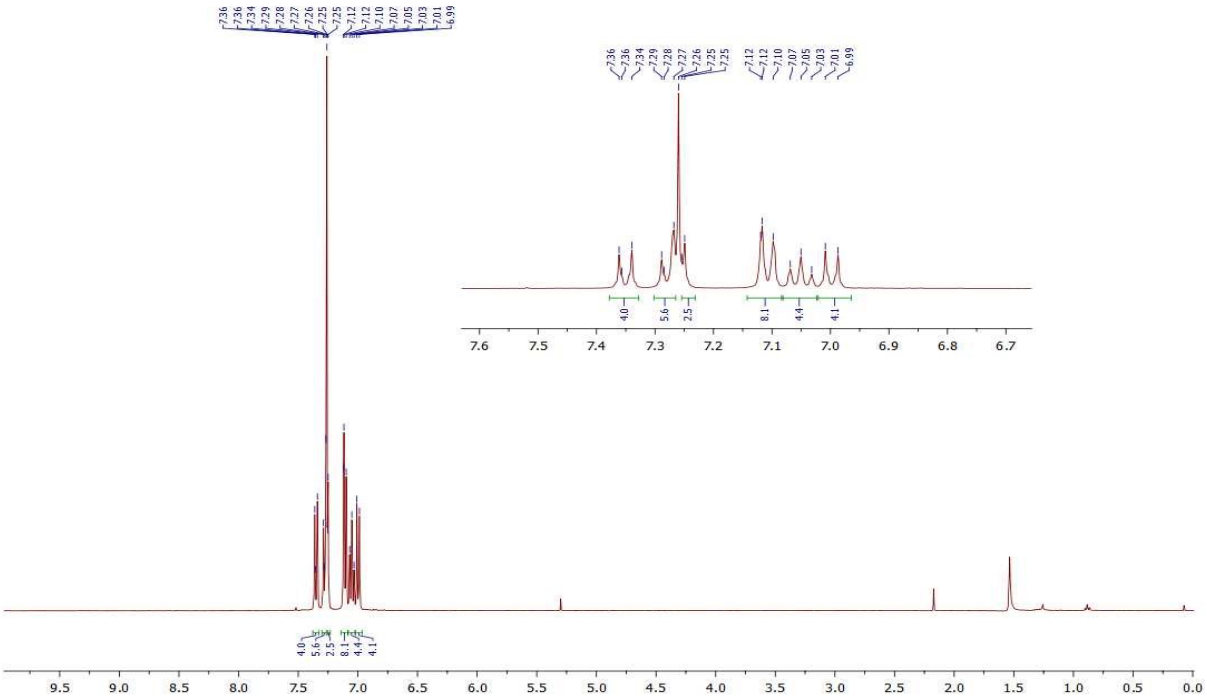

*Figure S1: ^{1}H NMR ($CDCl_3$, 400MHz) spectrum of **1a***

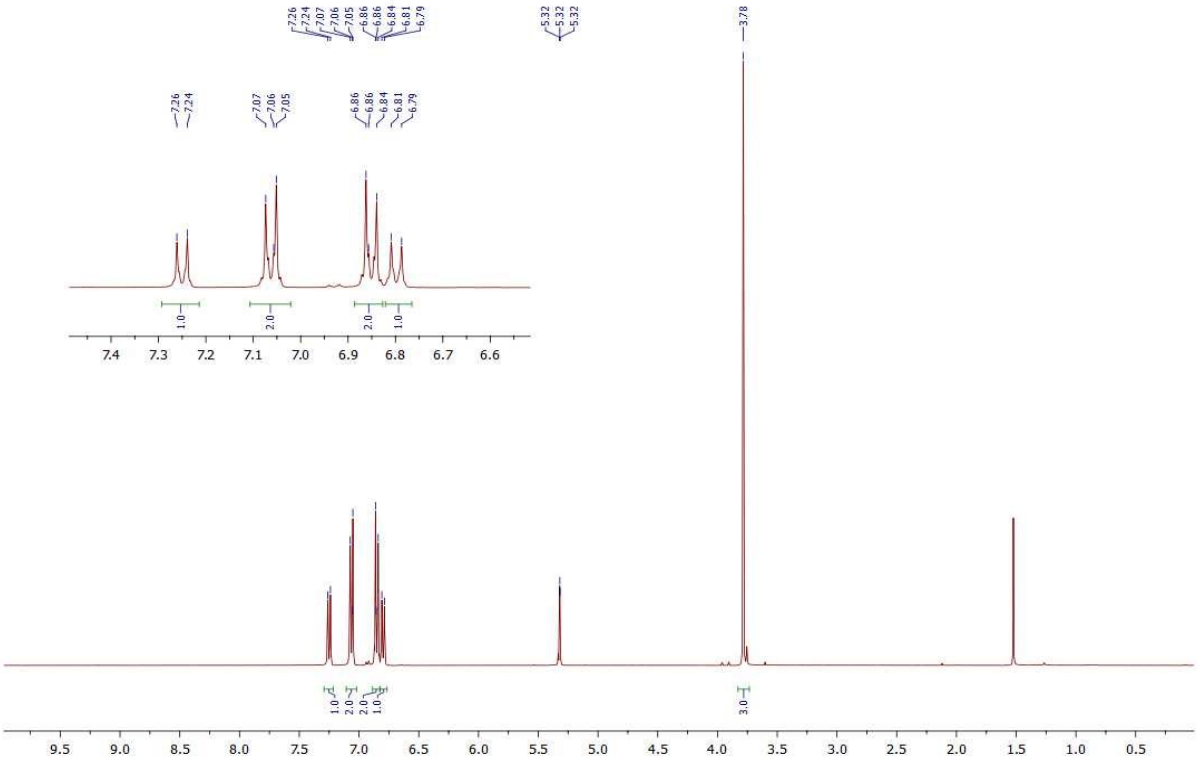

*Figure S2: ^{1}H NMR (CD_2Cl_2, 400MHz) spectrum of **1b***

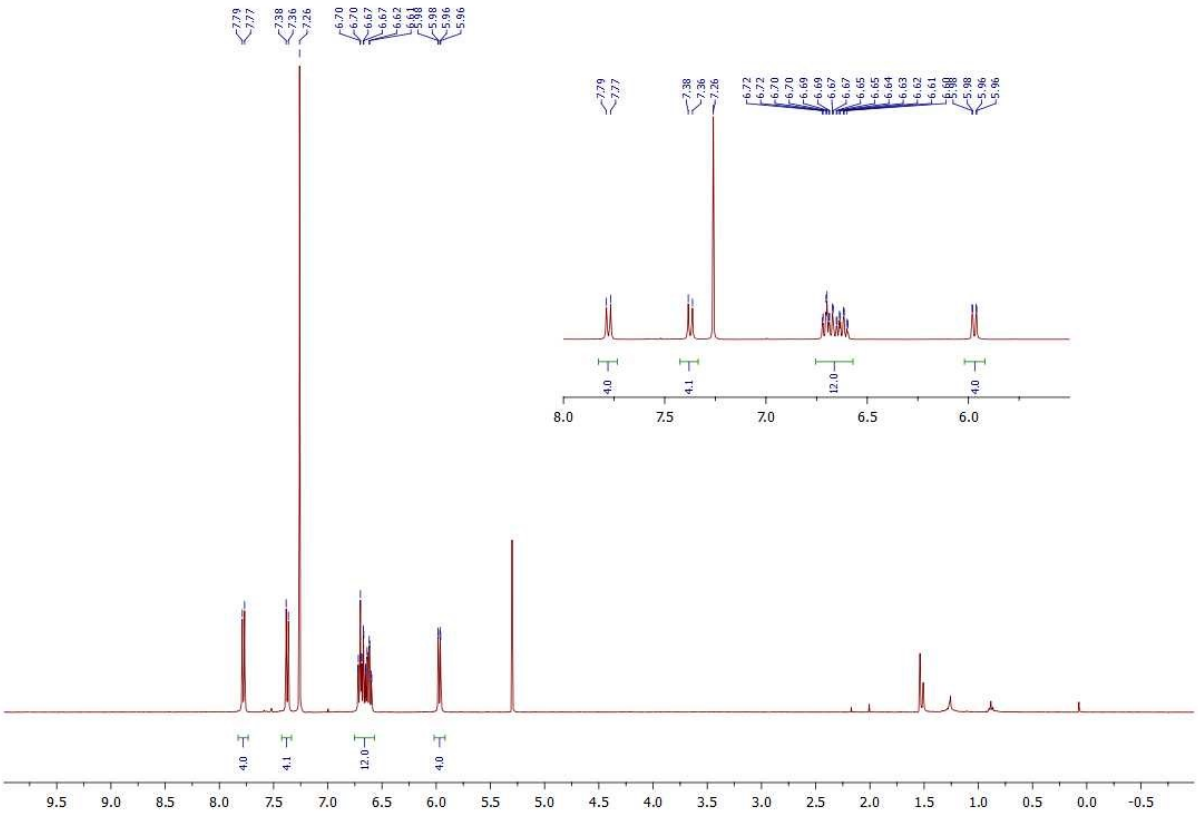

*Figure S3: ^{1}H NMR ($CDCl_3$, 400MHz) spectrum of **1c***

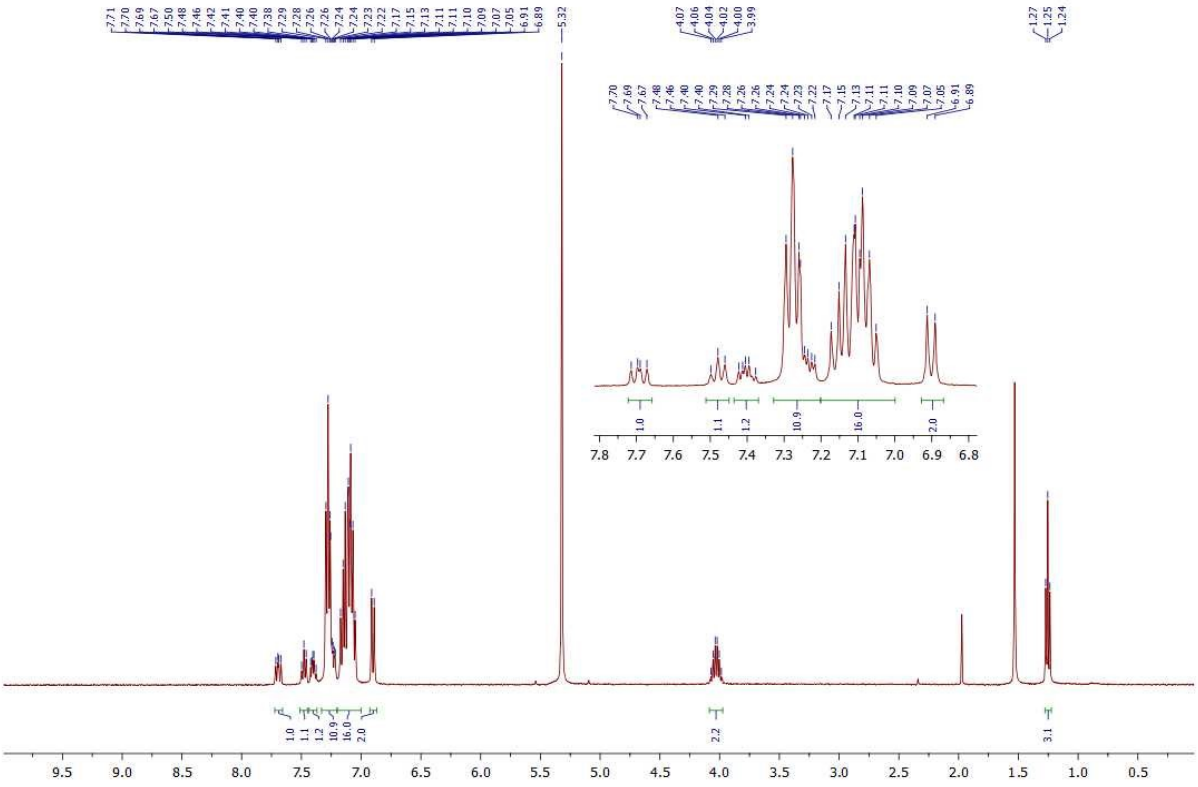

*Figure S4: ^{1}H NMR (CD_2Cl_2, 300MHz) spectrum of compound **2a***

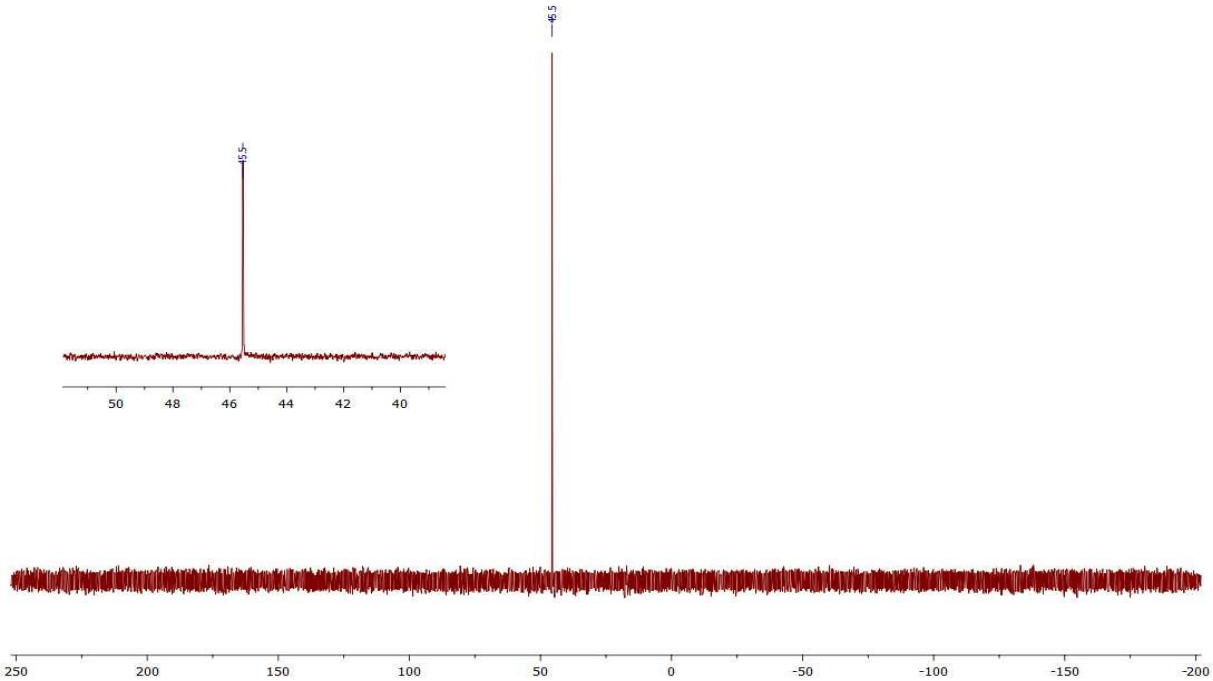

*Figure S5: ^{31}P (CD_2Cl_2, 162MHz) NMR spectrum of compound **2a***

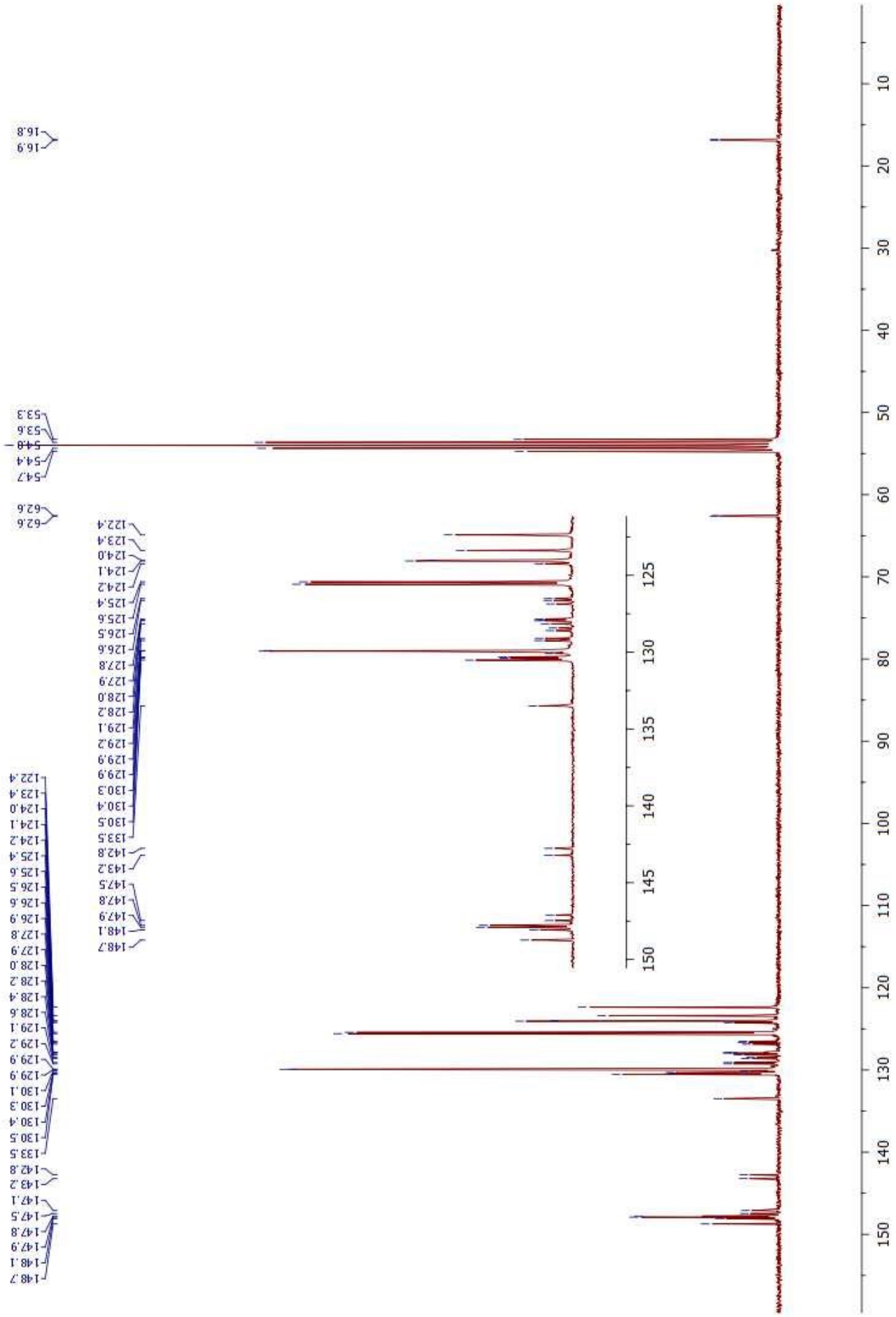

*Figure S6: ^{13}C NMR (CD_2Cl_2, 75MHz) spectrum of compound **2a***

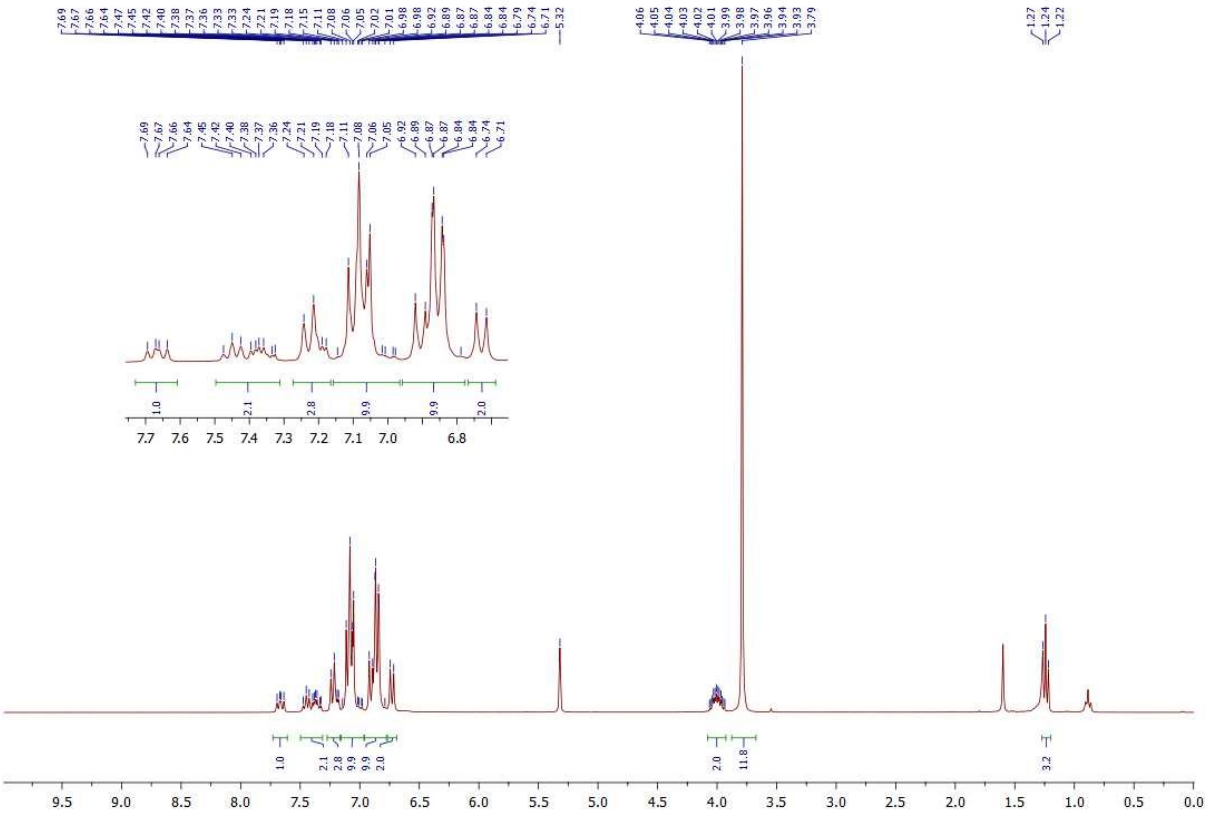

*Figure S7: ^{1}H NMR (CD_2Cl_2, 300MHz) spectrum of compound **2b***

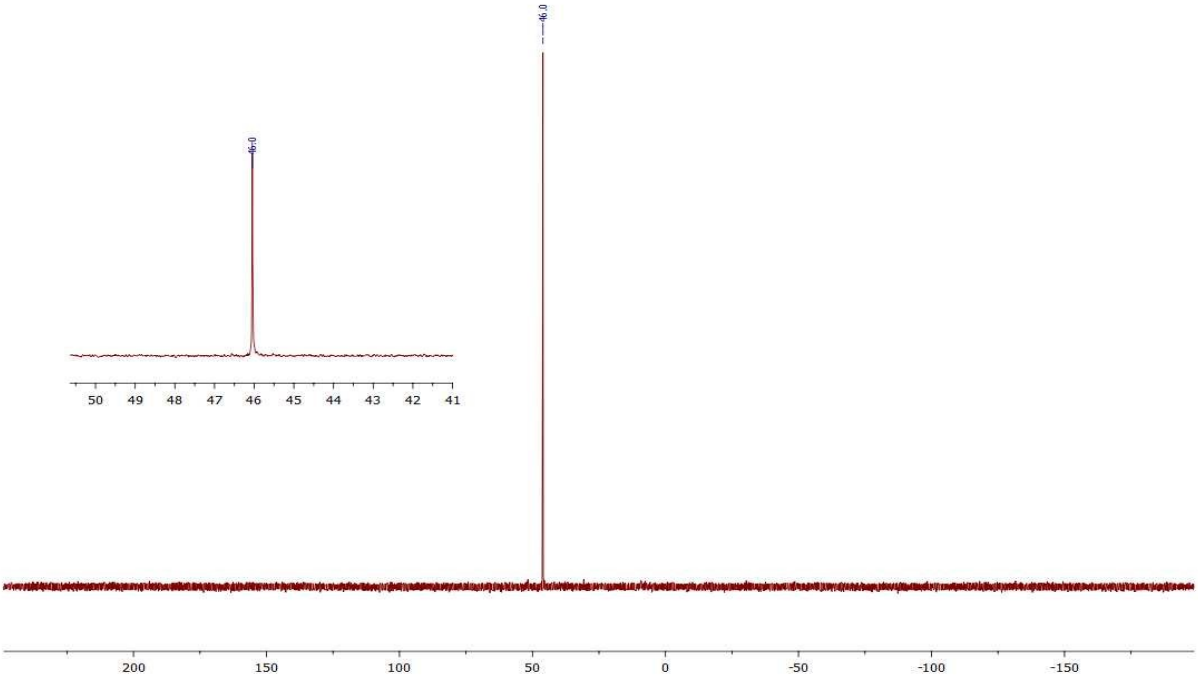

*Figure S8: ^{31}P (CD_2Cl_2, 162MHz) NMR spectrum of compound **2b***

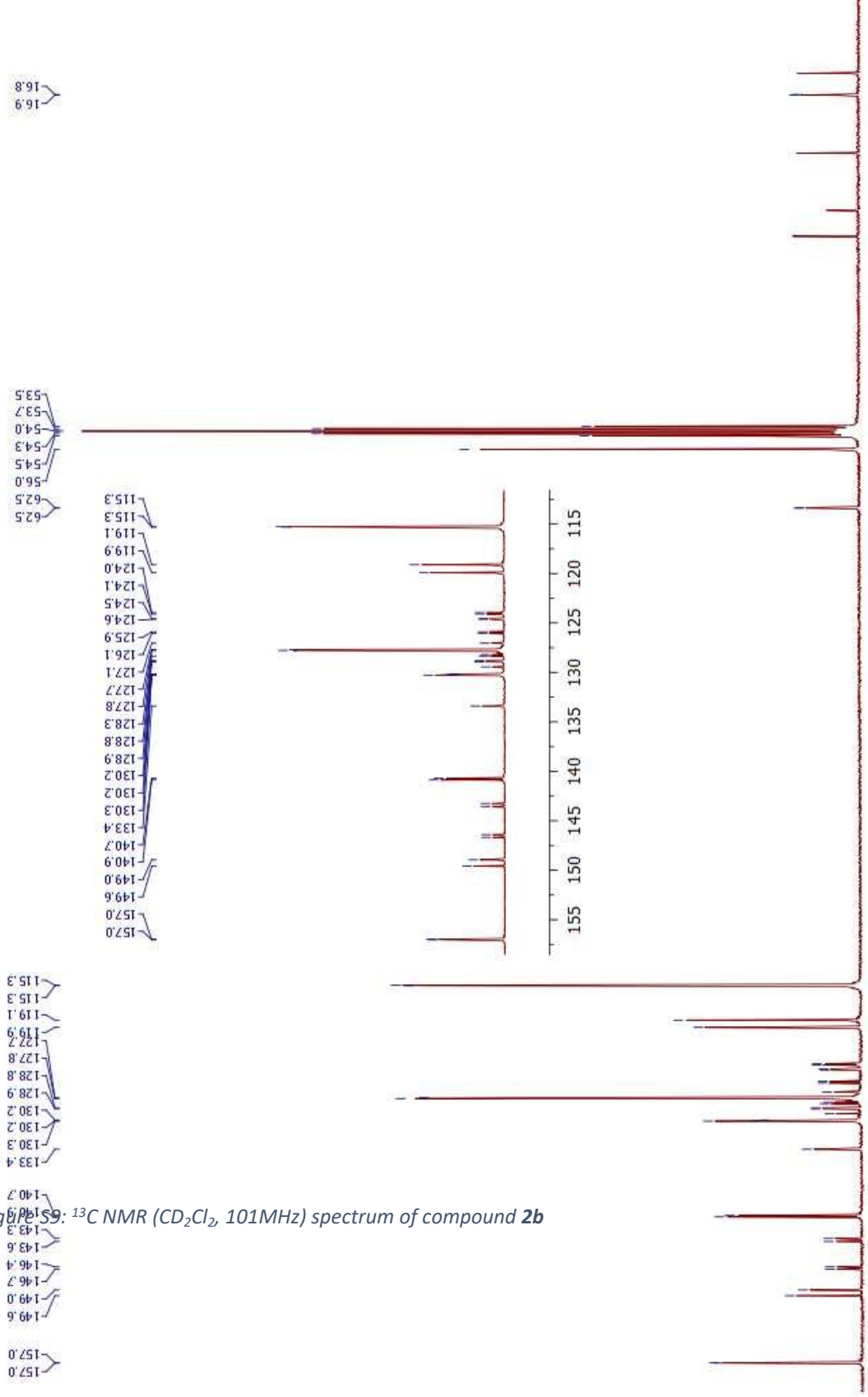

*Figure S9: ^{13}C NMR (CD_2Cl_2, 101MHz) spectrum of compound **2b***

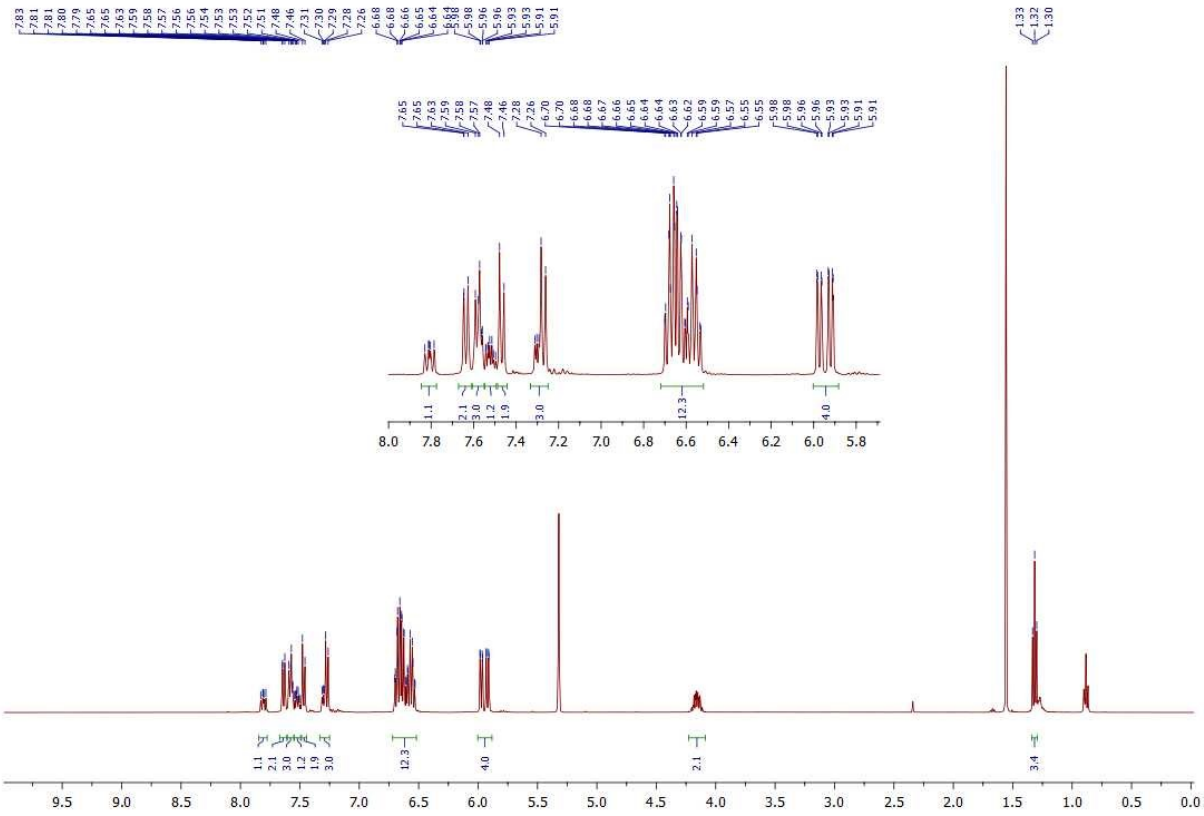

*Figure S10: ^{1}H NMR (CD_2Cl_2, 400MHz) spectrum of compound **2c***

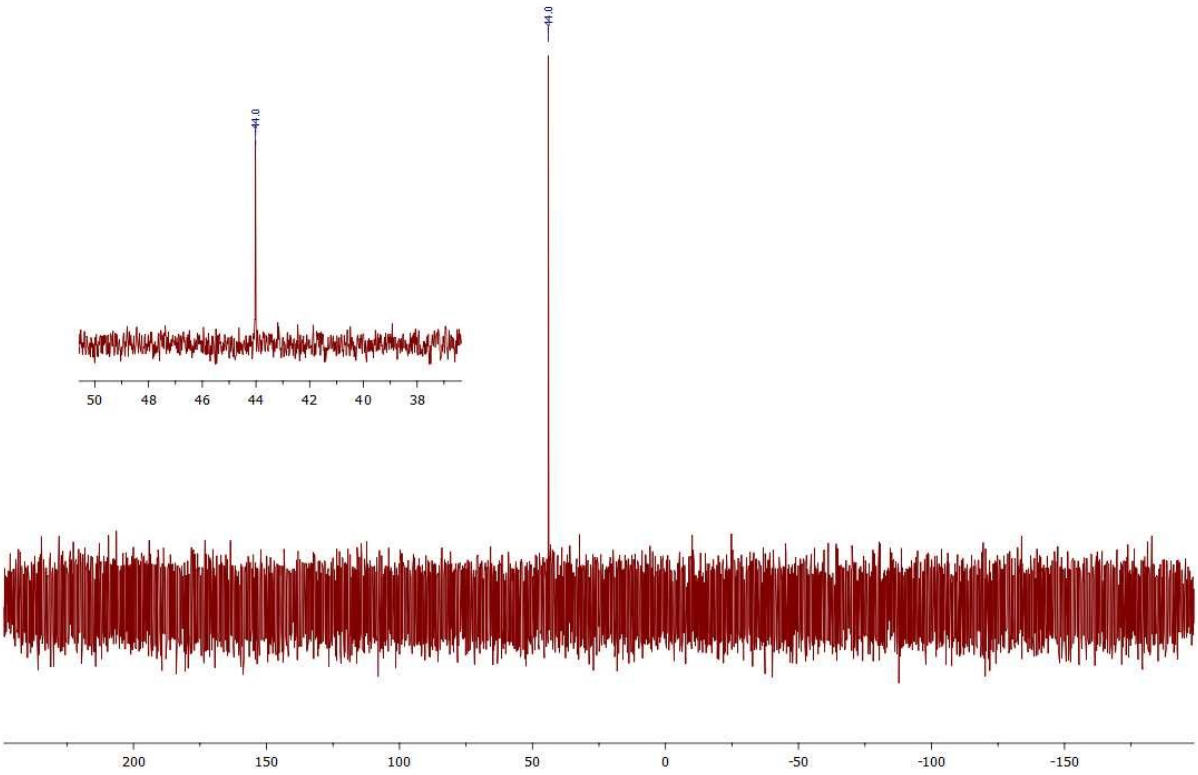

*Figure S11: ^{31}P NMR (CD_2Cl_2, 162MHz) spectrum of compound **2c***

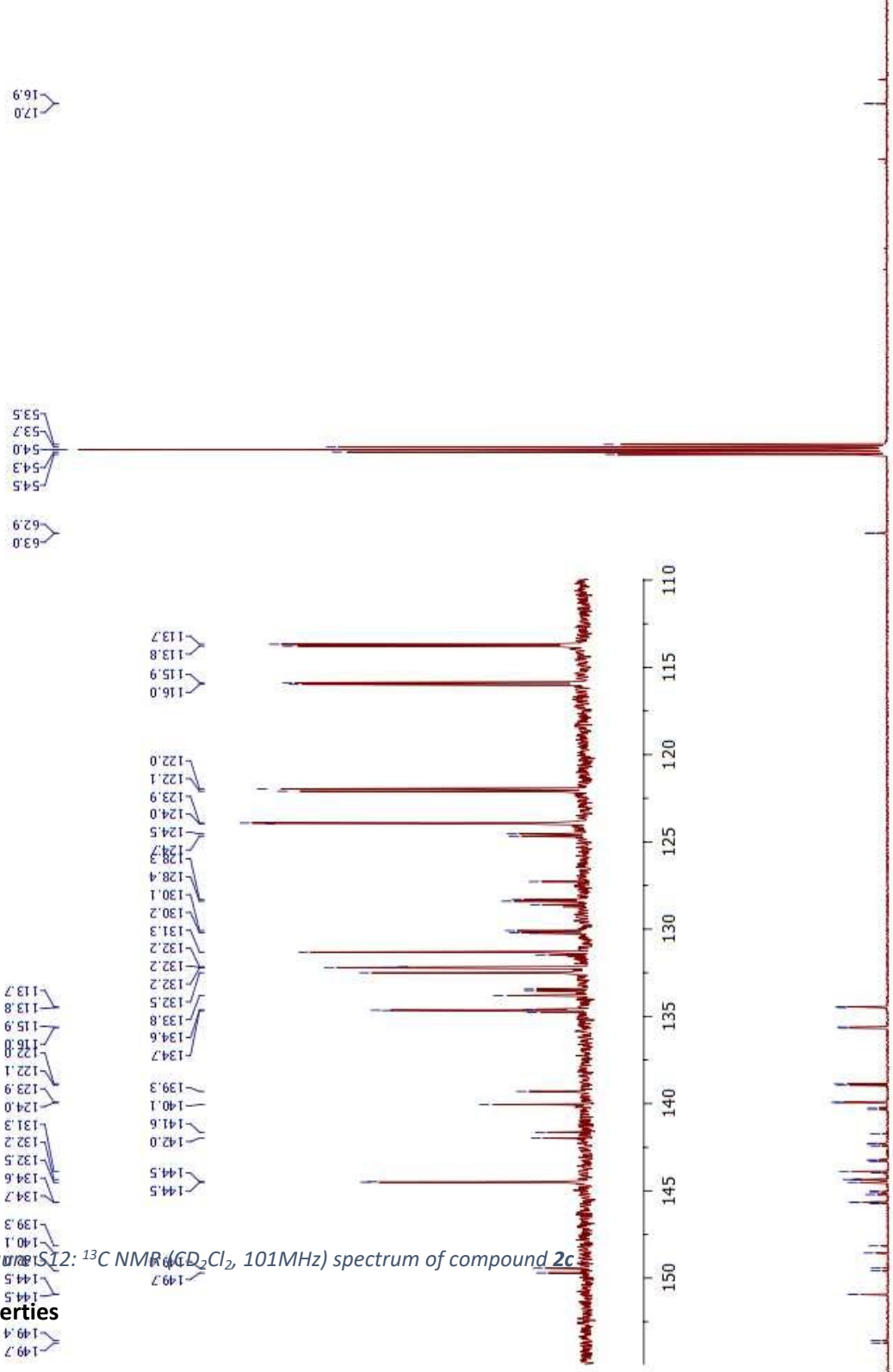

*Figure S12: ^{13}C NMR (CD_2Cl_2, 101MHz) spectrum of compound **2c***

Optical and Redox Properties

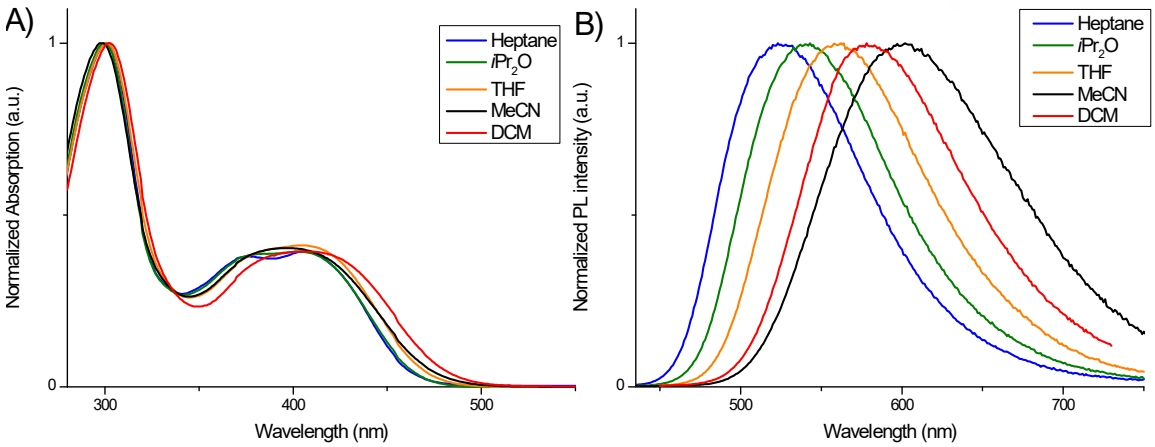

*Figure S13: A) Normalized absorption spectra of **2a** in various solvents (c ≈ 1.10^{-5}mol.L^{-1}) B) Normalized emission spectra of **2a** in various solvents (c ≈ 1.10^{-5}mol.L^{-1})*

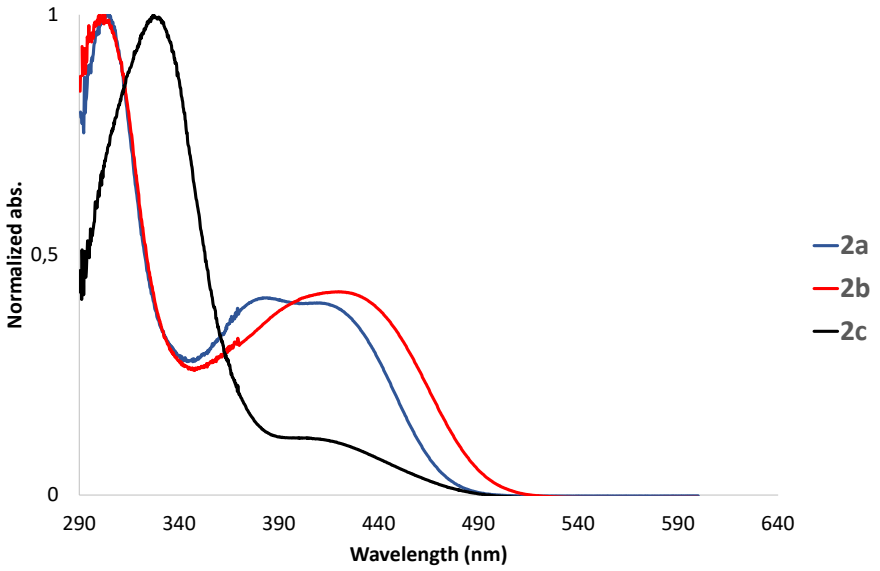

Fig S14: Normalized Absorption spectra of **2a-c** in toluene (c ≈ 1.10^{-6} M).

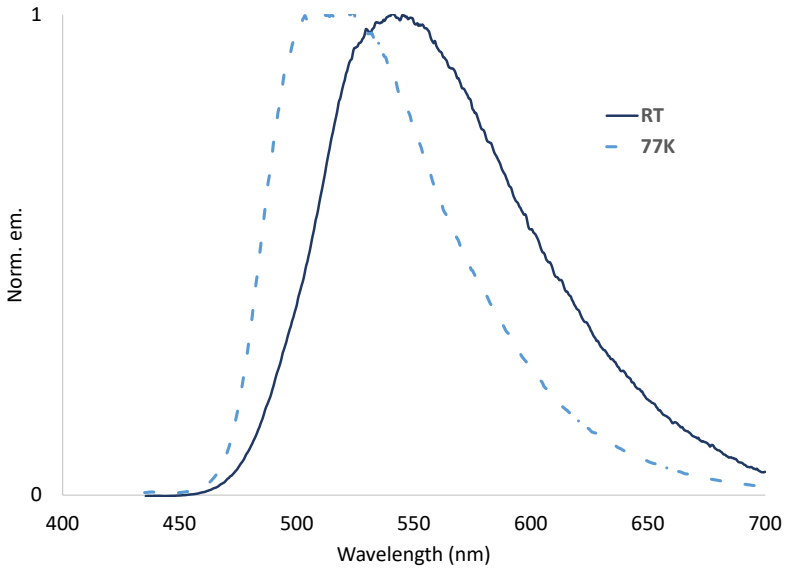

Fig S15: Normalized emission of **2a** in diluted toluene at RT and 77K.

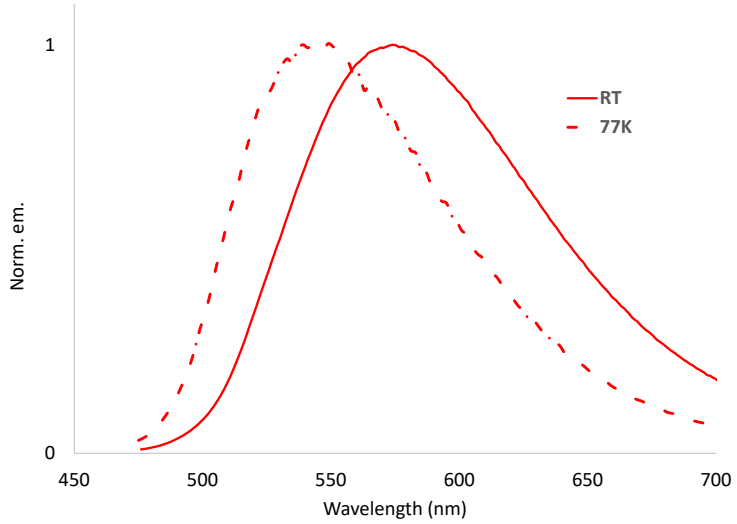

Fig S16: Normalized emission of **2b** in diluted toluene at RT and 77K.

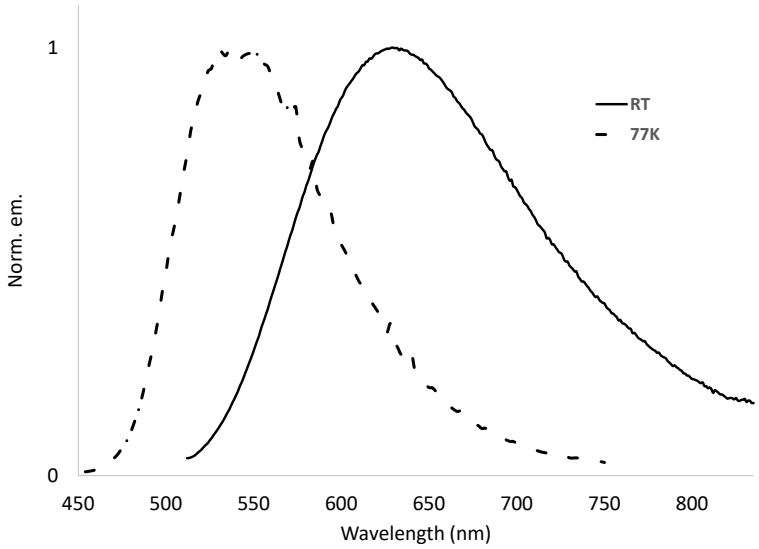

Fig S17: Normalized emission of **2c** in diluted toluene at RT and 77K.

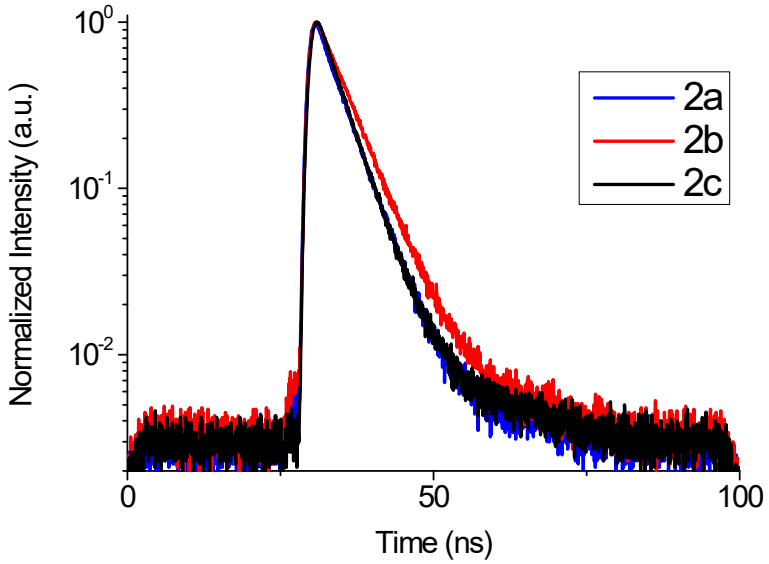

Fig S18: Normalized transient PL decay of **2a-c** in toluene solution at RT.

Table S1: photophysical data in diluted toluene

	λ_{abs} [a] (nm)	λ_{em} [a] (nm)	τ (ns)
2a	302, 383, 414	544	4.1(42%) 7.6(58%)
2b	301, 420	576	3.8(59%) 6.4(41%)
2c	329, 407	630	6.3 (48%) 14.3(52%)

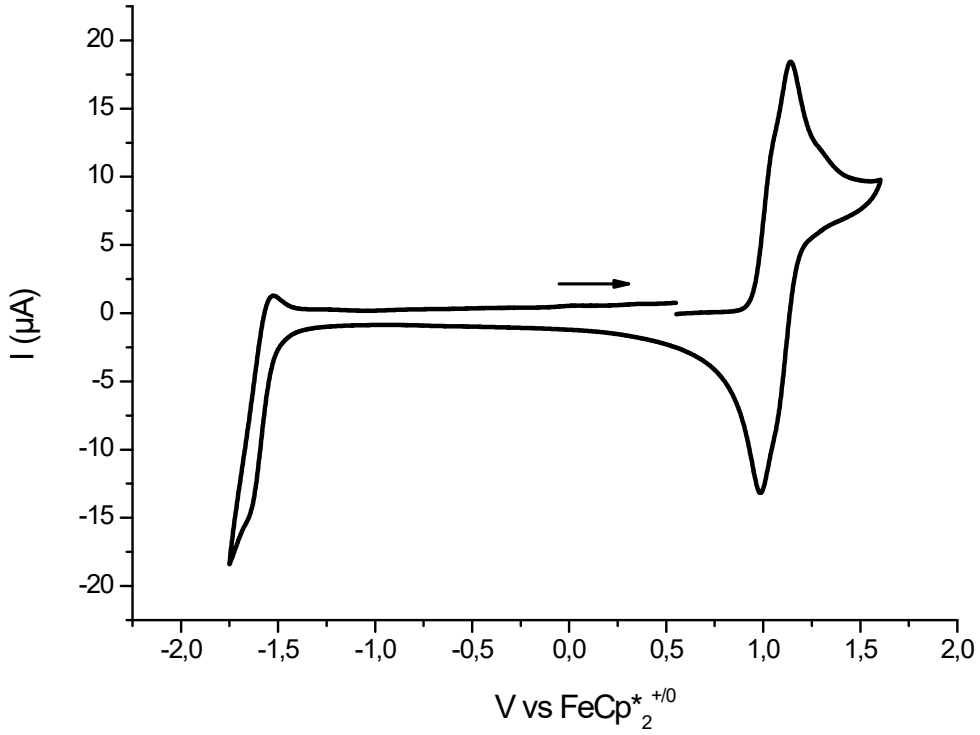

*Figure S19: Cyclic voltammetry (200mV.s^{-1}) of **2a** in DCM at room temperature. Decamethylferrocene used as internal standard.*

$E_{ox}(1/2)$ = +1.06V $E_{red}(1/2)$ = -1.59V E_{ox}(onset) = +0.95V E_{red}(onset) = -1.52V

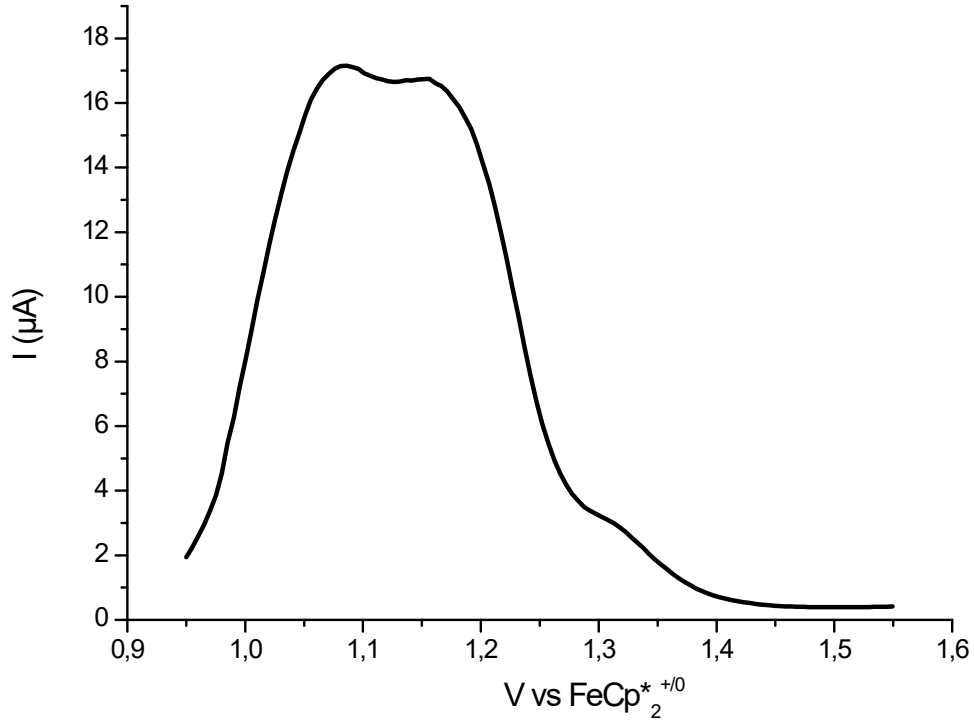

*Figure S20: Differential Pulse Voltammetry of **2a** in DCM at room temperature. Decamethylferrocene used as standard.*

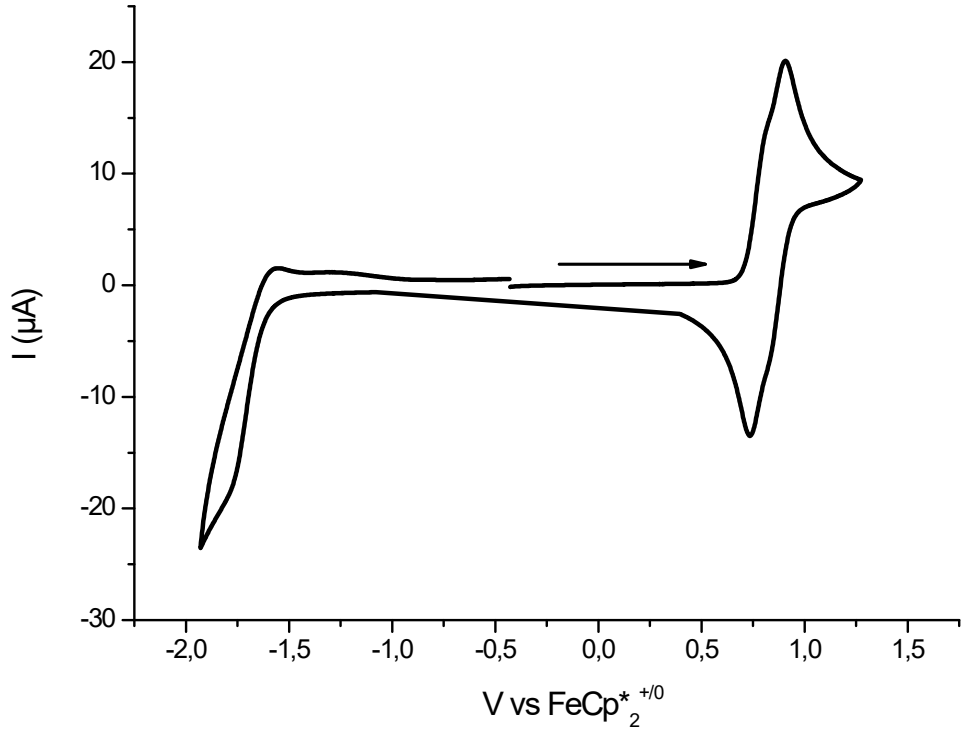

*Figure S21: Cyclic voltammetry (200mV.s^{-1}) of **2b** in DCM at room temperature. Decamethylferrocene used as internal standard.*

E_{ox}(1/2) = +0.83V E_{red}(1/2) = -1.70V E_{ox}(onset) =+0.71V E_{red}(onset) = -1.62V

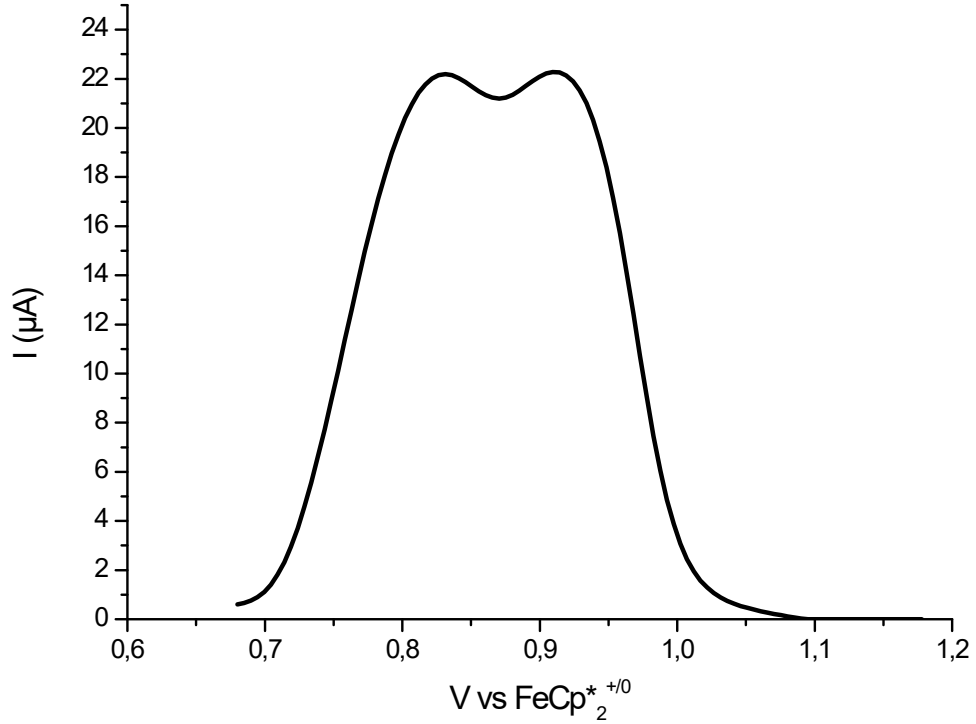

*Figure S22: Differential Pulse Voltammetry of **2b** in DCM at room temperature. Decamethylferrocene used as standard.*

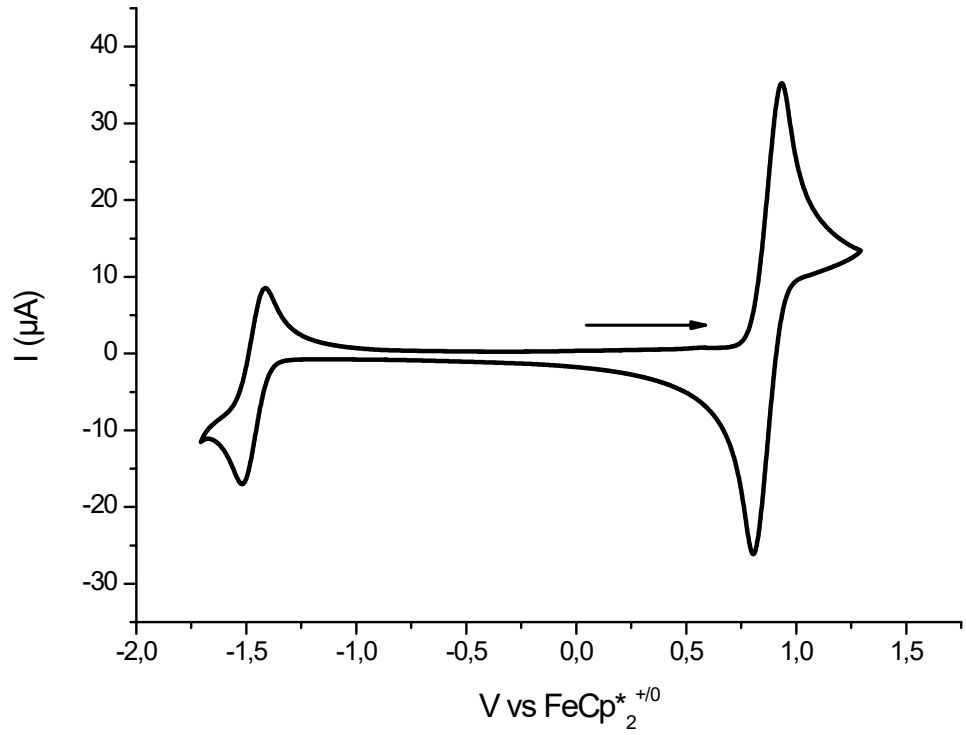

*Figure S23: Cyclic voltammetry (200mV.s^{-1}) of **2c** in DCM at room temperature. Decamethylferrocene used as internal standard.*

$E_{ox}(1/2)$ = +0.87V $E_{red}(1/2)$ = -1.46V E_{ox}(onset) = -1.40V E_{red}(onset) = +0.80V

Computational details

We have considered complete structure for all dyes. We used a computational strategy relying on TD-DFT combined with the popular Polarizable Continuum Model (PCM)[5] for simulating solvent effects (DCM here). All calculations were achieved with the Gaussian16.A03 program,[6] with improved self-consistent field (10^{-10} a.u.) and geometry optimization (10^{-5} a.u.) thresholds. The DFT and TD-DFT calculations use Truhlar's M06-2X *meta*-GGA hybrid functional,[7] a choice justified as this functional tends to provide consistent (high correlation) energies with respect to experimental data. Following our approach, the 6-31G(d) atomic basis set was selected for geometries and vibrations whereas the 6-31+G(d,p) basis set is chosen for obtaining total and transition energies. We have optimized and computed frequencies on both the ground and excited states, and the no imaginary frequency was found. All our TD-DFT energies rely on the LR+cLR solvation model,[8] so as to be as general as possible in the modelling of environmental effects.

To estimate the S-T gaps, we used the SCS-CC2,[9] approach as implemented in the Turbomole 7.3 code.[10] The SCS-CC2 singlet and triplet excited energies were calculated in gas phase, using the aug-cc-pVDZ atomic basis set, and applying the resolution of identity scheme. These calculations were performed on the S1 optimal geometries obtained by TD-DFT as explained above. Note that the use of SCS-CC2 for S-T gap has been reported to yield very accurate estimates as compared to experimental values.[11]

OLEDs devices

The OLED devices were fabricated onto indium tin oxide (ITO) glass substrates purchased from Xin Yang Technology (90 nm thick, sheet resistance of 15 Ω/□). Prior to organic layer deposition, the ITO substrates were cleaned by sonication in a detergent solution, rinsed twice in de-ionized water and then in isopropanol solution and finally treated with UV-ozone during 15 minutes. The OLEDs stack used is: Glass / ITO / CuPc (10 nm) / α-NPB (40 nm) / EML (20 nm) / TPBi (40 nm) / LiF (1.2 nm) / Al (100 nm). Copper II phthalocyanine (CuPc) is used as hole injection layer (HIL), N, N'-Bis-(1-naphthalenyl)- N,N'-bis-phenyl-(1,1'-biphenyl)-4,4'-diamine (αNPB) as hole transport layer (HTL), 1,3,5-Tri(m-pyridin-3-ylphenyl) 2,2',2"-(1,3,5-Benzinetriyl)-tris(1-phenyl-1-H-benzimidazole) (TPBi) as electron transport layer (ETL), lithium fluoride as electron injection layer (EIL) and 100 nm of aluminum as the cathode, respectively. The emitting layer (EML) is a host-guest system of 20 nm thick with 4,4'-bis(2,2'-diphenylvinyl)biphenyl (DPVBi) as the host and molecule **2a-c** as the guest (doping ratio 1-100% weight). Organic layers were sequentially deposited onto the ITO substrate at a rate of 0.2 nm/s under high vacuum (10^{-7} mbar). The doping rate was controlled by simultaneous co-evaporation of the host and the dopant. An in-situ quartz crystal was used to monitor the thickness of the layer depositions with an accuracy of 5%. The active area of the devices defined by the Al cathode was 0.3 cm^2. The organic layers and the LiF/Al cathode were deposited in a one-step process without breaking the vacuum. After deposition, all the measurements were performed at rt and under ambient atmosphere with no further encapsulation of devices. The current–voltage–luminance (I–V–L) characteristics of the devices were measured with a regulated power supply (ACT100 Fontaine) combined with a multimeter (Keithley) and a 1 cm^2 area silicon calibrated photodiode (Hamamatsu). Electroluminescence (EL) spectra and chromaticity coordinates of the devices were recorded with a PR650 SpectraScan spectrophotometer, with a spectral resolution of 4 nm

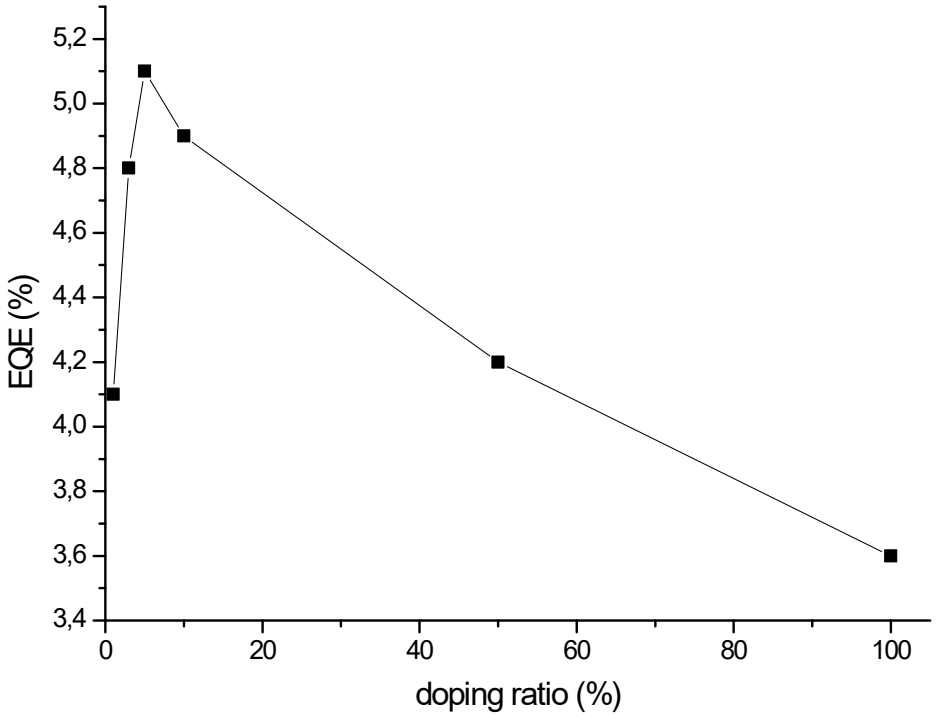

*Figure S24: Evolution of the EQE of **2a** OLED device versus the doping rate of emitter in dPVBi*

Table S2

Doping rate	Φ_{PL}(**2a**) (%)	Φ_{PL}(**2b**) (%)	Φ_{PL}(**2c**) (%)
5% in dPVBi	93	85	36
pure	90	54	16

Absolute photoluminescence quantum yield of **2a-c** sublimated film as pure emitter or at 5% in dPVBi.

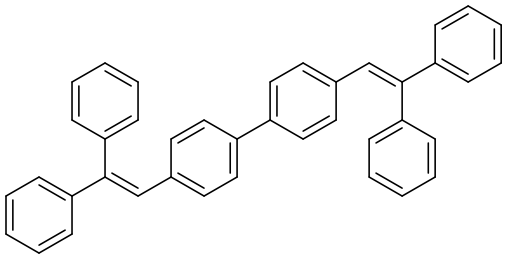

Figure S25: Chemical structure of dPVBi

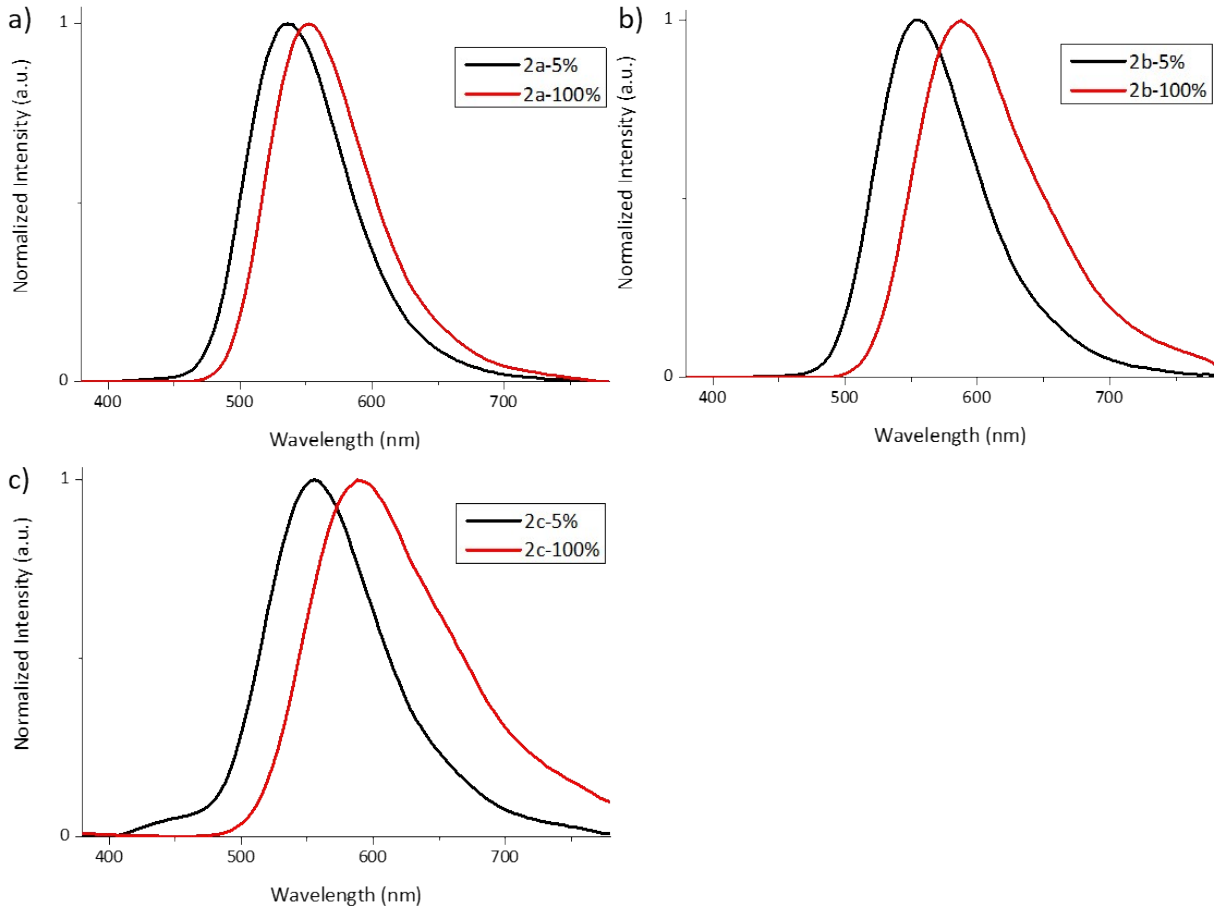

*Figure S26: Normalized electroluminescence (at 30 mA.cm^{-2}) spectra of OLED containing a) **2a**, b) **2b** and c) **2c**. The black curves indicate a doping rate of 5% in DPVBi and the red curves indicate a doping rate of 100% (only emitter in the EML).*

(1) Kuo, L. Y.; Baker, D. C.; Dortignacq, A. K.; Dill, K. M. Phosphonothioate Hydrolysis by Molybdocene Dichlorides: Importance of Metal Interaction with the Sulfur of the Thiolate Leaving Group. *Organometallics* **2013**, *32* (17), 4759–4765. https://doi.org/10.1021/om400382u.
(2) Li, Q.; Li, Y.; Min, T.; Gong, J.; Du, L.; Phillips, D. L.; Liu, J.; Lam, J. W. Y.; Sung, H. H. Y.; Williams, I. D.; Kwok, R. T. K.; Ho, C. L.; Li, K.; Wang, J.; Tang, B. Z. Time-Dependent Photodynamic Therapy for Multiple Targets: A Highly Efficient AIE-Active Photosensitizer for Selective Bacterial Elimination and Cancer Cell Ablation. *Angew. Chem.* **2019**, ange.201909706. https://doi.org/10.1002/ange.201909706.
(3) Kou, C.; Feng, S.; Li, H.; Li, W.; Li, D.; Meng, Q.; Bo, Z. Molecular "Flower" as the High-Mobility Hole-Transport Material for Perovskite Solar Cells. *ACS Appl. Mater. Interfaces* **2017**, *9* (50), 43855–43860. https://doi.org/10.1021/acsami.7b13380.
(4) He, Z.; Cai, X.; Wang, Z.; Li, Y.; Xu, Z.; Liu, K.; Chen, D.; Su, S.-J. Sky-Blue Thermally Activated Delayed Fluorescence Material Employing a Diphenylethyne Acceptor for Organic Light-Emitting Diodes. *J. Mater. Chem. C* **2018**, *6* (1), 36–42. https://doi.org/10.1039/C7TC02763J.
(5) Tomasi, J.; Mennucci, B.; Cammi, R. Quantum Mechanical Continuum Solvation Models. *Chem. Rev.* **2005**, *105* (8), 2999–3094. https://doi.org/10.1021/cr9904009.
(6) Frisch, M. J.; Trucks, G. W.; Schlegel, H. B.; Scuseria, G. E.; Robb, M. A.; Cheeseman, J. R.; Scalmani, G.; Barone, V.; Petersson, G. A.; Nakatsuji, H.; Li, X.; Caricato, M.; Marenich, A. V.; Bloino, J.; Janesko, B. G.; Gomperts, R.; Mennucci, B.; Hratchian, H. P.; Ortiz, J. V.; Izmaylov, A. F.; Sonnenberg, J. L.; Williams-Young, D.; Ding, F.; Lipparini, F.; Egidi, F.; Goings, J.; Peng, B.; Petrone, A.; Henderson, T.; Ranasinghe, D.; Zakrzewski, V. G.; Gao, J.; Rega, N.; Zheng, G.; Liang, W.; Hada, M.; Ehara, M.; Toyota, K.; Fukuda, R.; Hasegawa, J.; Ishida, M.; Nakajima, T.; Honda, Y.; Kitao, O.; Nakai, H.; Vreven, T.; Throssell, K.; Montgomery, J. A., Jr.; Peralta, J. E.; Ogliaro, F.; Bearpark, M. J.; Heyd, J. J.; Brothers, E. N.; Kudin, K. N.; Staroverov, V. N.; Keith, T. A.; Kobayashi, R.; Normand, J.; Raghavachari, K.; Rendell, A. P.; Burant, J. C.; Iyengar, S. S.; Tomasi, J.; Cossi, M.; Millam, J. M.; Klene, M.; Adamo, C.; Cammi, R.; Ochterski, J. W.; Martin, R. L.; Morokuma, K.; Farkas, O.; Foresman, J. B.; Fox, D. J. Gaussian˜16 Revision C.01, 2016.
(7) Zhao, Y.; Truhlar, D. G. The M06 Suite of Density Functionals for Main Group Thermochemistry, Thermochemical Kinetics, Noncovalent Interactions, Excited States, and Transition Elements: Two New Functionals and Systematic Testing of Four M06-Class Functionals and 12 Other Functionals. *Theor. Chem. Acc.* **2008**, *120* (1–3), 215–241. https://doi.org/10.1007/s00214-007-0310-x.
(8) Vérité, P. M.; Guido, C. A.; Jacquemin, D. First-Principles Investigation of the Double ESIPT Process in a Thiophene-Based Dye. *Phys Chem Chem Phys* **2019**, *21* (5), 2307–2317. https://doi.org/10.1039/C8CP06969G.
(9) Hellweg, A.; Grün, S.; Hättig, C. *Phys. Chem. Chem. Phys*. **2008**, 10, 1159−1169.
(10) TURBOMOLE V7.3, a development of University of Karlsruhe and Forschungszentrum Karlsruhe GmbH, 1989−2007; TURBOMOLE GmbH. http://www.turbomole.com.
(11) Pershin,A.; Hall, D.; Lemaur, V.; Sanchi-Garcia, J. C.; Muccioli, L.; Zysman-Colman, E.; Beljonne, D.; Olivier, Y. *Nature Comm*. **2019**, 10, 597